Optical Properties of (C2H5C6H4NH2)2ZnBr2 Complex: Experimental and Quantum Chemical Studies

Asmaa Harmouzi, Mohammed Bouachrine, Philippe Guionneau, Alexandre Fargues, Abdesselam Belaaraj

Optical properties of (C2H5-C6H4-NH2)2ZnBr2 complex material: Experimental and TD-DFT studies

Asmaa Harmouzi[a], Mohammed Bouachrine[b], Philippe Guionneau[c], Alexandre Fargues[c], Abdesselam Belaaraj[a]

[a] Laboratoire de Physique des matériaux et modélisation des Systèmes, CNRST-URAC 08, Faculté des Sciences, Université Moulay Ismail, 50000-Meknès, Morocco.
[b] Equipe Matériaux, Environnement et Modélisation, Ecole Supérieure de Technologie, Université Moulay Ismail, 50040-Meknès, Morocco/ Molecular Chemistry and Natural Substances Laboratory, Faculty of Science, University Moulay Ismail, Meknes, Morocco
[c] CNRS, Univ. Bordeaux, ICMCB, UMR 5026, 87 avenue du Dr A. Schweitzer, F-33608 Pessac, France.

Abstract

This study aims to develop a new type of semiconductor materials. In this context, the coordination complex (CH_3-CH_2-C_6H_4-NH_2) $_2$ $ZnBr_2$ material was subjected to UV-Vis spectroscopy and the dependent theoretical density functional theory (TD-DFT) studies. The optical properties such optical absorption, band gap and molecular orbital energies are determined and discussed. The experimental results and theoretical conclusions appear to be in good agreement. Although we checked that the experimental molecular geometry is predicted correctly using the (TD-DFT) method. The molecular electrostatic potential (MEP) was calculated to predict physicochemical properties. The molecular composition of HOMO-LUMO and their band gap energies are represented in order to explain the activity of the title compound. So, the studied material seems to have a semiconductor behavior.

Keywords: Absorption bands; Frontier molecular orbitals; Band gap energy; TD-DFT.

1. Introduction

In the increasingly-wide context of research on inorganic-organic hybrid materials, and according to their important and diversified physicochemical properties originating in the association of the organic and inorganic properties [1], we currently focus on the design and investigation of coordination complexes [2-4]. Metal–organic coordination complexes, combining simple synthesis along with tunable optical properties had a lot of concern over the latest decades, due to their vast potential application in optoelectronic devices [5-7]. For example, with the relevant set of optoelectronic properties, metal–organic complexes may lead off to the next generation of solar energy conversion, replacing fragile and high-temperature processing semiconductor materials. The inorganic-organic coordination is completed at the level of the metal ion. Consequently, the Zn^{2+} ion has an electron configuration [Ar] 3d10; therefore, the coordination links are created by involvement of the unoccupied 4s and 4p AOs. By reason of the coordination, a quasi-tetrahedral complex of zinc is formed, corresponding bonds are represented in a simple way by the means of four electron pairs that occupy sp3 hybrid orbitals. From the optical point of view, there are two bands in the far UV corresponding to the ligand (R-NH_2) and one band corresponding to the transition of the metal to a ligand charge-transfer (MLCT) as well as two other bands which correspond to the transition from halogen to metal.
It is well known that the band gap energy between HOMO and LUMO is a decisive parameter in the determination of the electrical transport properties of molecules [8]. In addition, the band gap energy has effectively been of use to prove the bioactivity from intermolecular charge transfer [9, 10]. Furthermore, a molecular complex with a slight frontier orbital gap have higher

polarizability and it is mostly associated to a high chemical reactivity and a low kinetic stability [11]. In the present work, the optical properties of the complex dibromidobis(4-ethylaniline-kN)Zinc of chemical formula $(CH_3\text{-}CH_2\text{-}C_6H_4\text{-}NH_2)_2ZnBr_2$ (hereinafter called 4EA-$ZnBr_2$), like band gap energy, activation energy and absorption wavelength, are reported and discussed.Results and Discussion

2. Experimental optical study

The UV-Vis diffuse absorbance spectroscopy (Figure 1) was performed on a crystalline powder of the 4EA-$ZnBr_2$ structure of a previous work [2] at room temperature, on a VARIAN Cary 5000 double beam spectrophotometer in the spectral range 200-800 nm. The absorption spectrum F(R) calculated from the reflectance R spectrum using the Kubelka-Munk function: $F(R) = (\alpha/S)\,(1-R)^2/(2R)$. Where α, S are respectively the absorption and scattering coefficients [12.13].

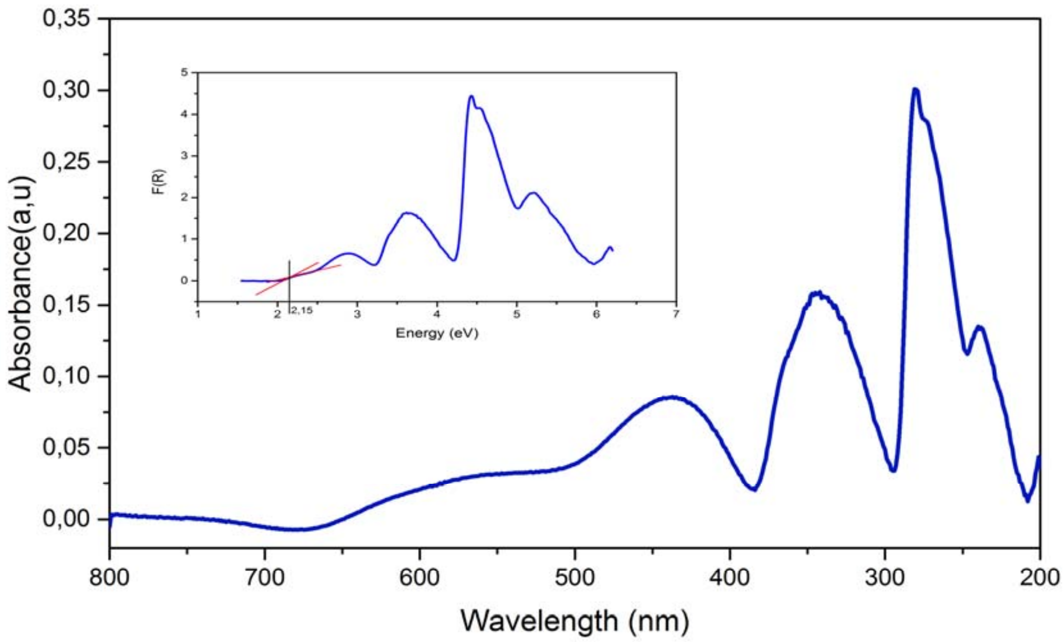

Figure1: UV-vis absorption spectrum of 4EA-$ZnBr_2$

Figure 1 shows the UV-visible absorption spectrum of 4EA-$ZnBr_2$ measured at room temperature. Five strongest absorption bands centered at 236, 275, 338, 425 nm and 580 nm, are observed. The high intense absorption peak at 236 nm is due to (π→π*) electronic transition while the second peak at 275 nm is due to (n→π*) electronic transition. So the intense band in the visible region is assigned the metal to ligand charge-transfer (MLCT) [14] which is associated with Zn(II)-4ethylaniline (λ=338nm).This metal to ligand charge transfer transition arises from the (t2g6) on the Zn(II) to the empty π* orbitals on 4-Ethylaniline ligands (t2g6 → π *) [15-17]. The peak at 580 nm is attributed to the transition from the initial electronic state of the Br-3p valence band to the Zn-4p. The second peak at 425nm comes from the transition between the Br-3p valence band and Zn-4s conduction band [18-20]. We have also determined the band gap by transformed Kubelka-Munk spectrum (Figure 1) and the photon energy axis. The obtained value is found to be about 2.15 eV, which agrees very well with that of the hybrid perovskite compound $CH_3NH_3SnBr_3$ [21]. This result indicates that the studied compound is a wide band gap semiconductor.

3. Optical properties calculations

To determine the structural and optoelectronic characteristics of the studied molecule, we have started by optimizing the structure of this molecule using DFT quantum chemistry calculations and especially the Lee - Yang - Parr LYP (B3LYP) method [22- 26]. In the same vein, we have used the 6-311G base (d, p) [27] which is widely applied and cited by many authors for its effectiveness in the study of macromolecular systems [28]. A frequency calculation has been carried out to ensure that it is an absolute minimum corresponding to the most stable conformation. Electronic properties such as HOMO, LUMO and band gap energy are determined from the fully optimized structure.
The SCXRD experimental data [2] were used as a beginning point for optimizing the atomic positions. In order to determine the absorption properties and the electronic transitions, we have adopted the method of the functional theory of density versus time (TD-DFT) [29] starting from the optimized structure obtained by the B3LYP/6-311G base (d, p) method. All the quantum chemistry calculations performed in this work were done using the Gaussian (03) program [30]. The calculations of the simulated absorption spectra were realized using the SWIZARD program [31].

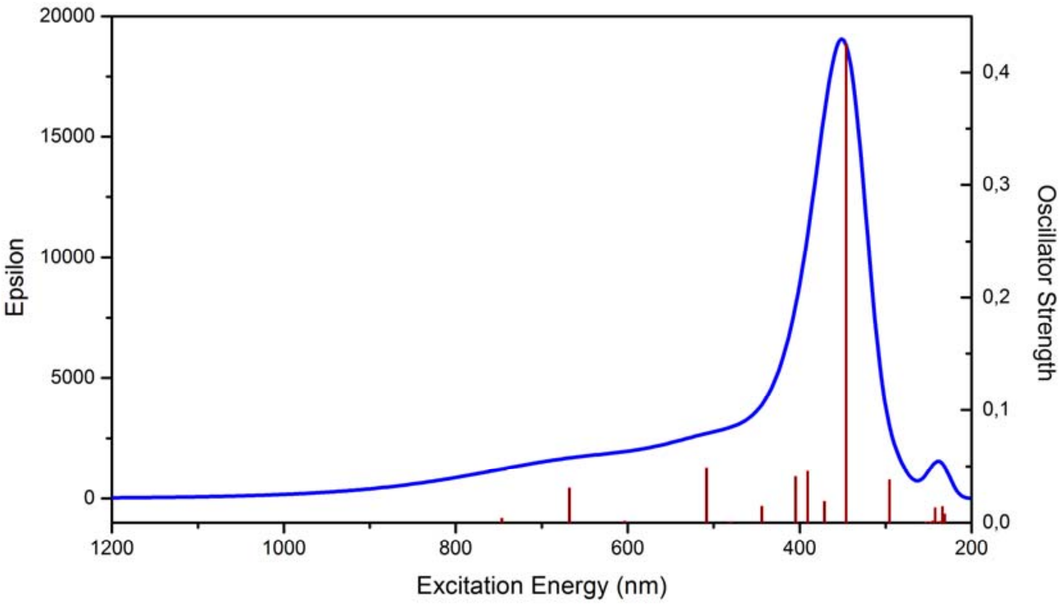

Figure 2: Simulated UV–Vis absorption spectrum of 4EA-$ZnBr_2$

The corresponding simulated UV–Vis absorption spectrum data (**Figure 2**) like energy of activation, wavelength absorption λabs (nm) and oscillator strength (O.S), calculated using TD/DFT theory are given in Table1, where MO is the molecular orbital. As it can be seen, the calculated wavelength λabs of the studied compound shows a maximum at 604.001, 445.215, 347.721, 294.008 and 236.542 nm. As illustrated in Table 1, this could be regarded as an electron transition process which is the reverse of the absorption corresponding respectively to H-2 ->LUMO, H-8 ->LUMO, H -9->LUMO, H-10 ->LUMO and H-2 ->L+1 electron transitions configurations. In addition, it is worth noting that the broader absorption peak means that there is a distribution of energy level corresponding to the π→π*, n - π* or halogen-metal transition. These interesting points are seen both from experimental and theoretical absorption results.

Table 1: Absorption spectra data obtained by TD-DFT methods at B3LYP/6-311 G (d,p) optimized geometry.

No.	Excitation energies (eV)	λmax(nm)	Oscillator Strengths	MO/character	% (Major contributions

3	2.053	604.001	0.002	H-2->LUMO	96
6	2.785	445.215	0.015	H-8->LUMO	13
10	3.566	347.721	0.426	H-9->LUMO	22
11	4.217	294.008	0.038	H-10->LUMO	88
19	5.241	236.542	0.015	H-2->LUMO+1	91

3.1 The molecular orbital study

The optimization of molecular geometry was made at B3LYP/6-311G (d,p) level in gas phase. The structure calculated is presented in Figure 3. So, to obtain an indication of excitation properties, the molecular orbital contribution of the complex materials must be understood, which explains the relative arrangement of the occupied and virtual orbits. As observed in Figure 4, the HOMO and LUMO are respectively an antibonding and binding character between the subunits.

Further, the electron distributions of HOMOs are essentially localized on conjugation spacer moiety between halogen and metal, but in the LUMOs both of them are distributed between metal and halogen and in the aromatic cycle. We present in Table 2 the calculated values of the HOMO/LUMO and band gap energies. The band gap energy (Eg) was evaluated theoretically as the difference between the HUMO and LOMO energies ($Eg = |E_{HOMO} - E_{LUMO}|$). The obtained value Eg= 2.22 eV agree very well with the experimental one, mentioned above, and confirms the semiconductor behavior of the studied compound.

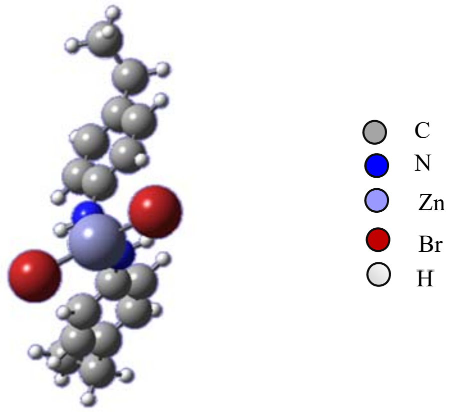

Figure 3: Optimized and theoretical molecular structure of 4EA-ZnBr$_2$ obtained at B3LYP/6-311G (d,p) level.

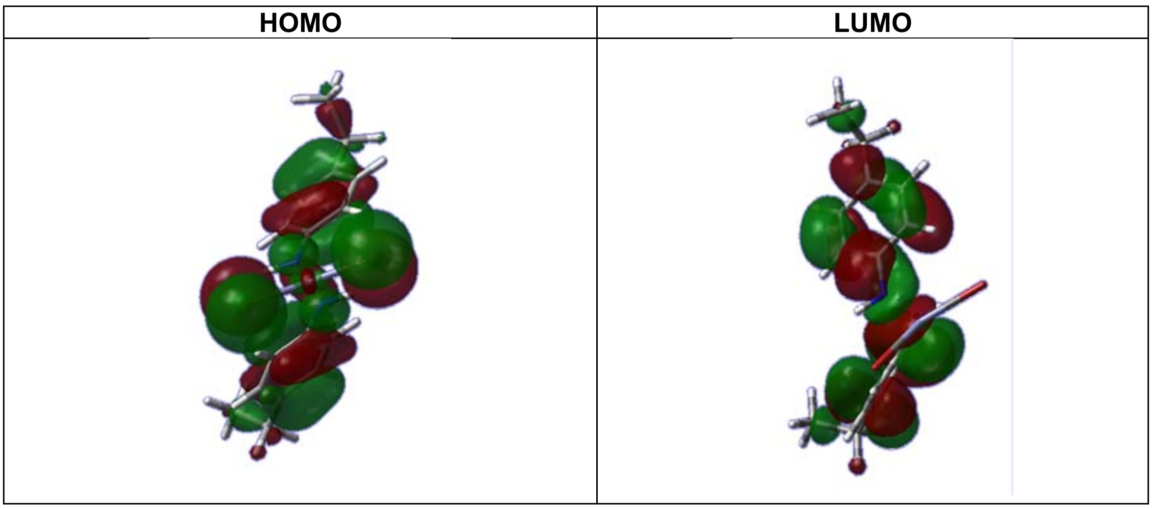

Figure 4: Obtained isodensity plots of the frontier orbital HOMO and LUMO of 4EA-ZnBr2 obtained at B3LYP/6-311G (d,p) level.

Table 2: The calculated values of the HOMO/LUMO energies and band gap energies for 4EA-ZnBr2.

E(HOMO) (eV)	E(LUMO) (eV)	Egap (eV)
-6.20	-3.98	2.22

3.2 Analysis of molecular electrostatic potential

In this part, we are interested in the study of the electrostatic molecular potential (MEP) in order to identify the reactive sites for the electrophilic and nucleophilic attack and to predict the physicochemical properties. We calculated Le (MEP) of the studied molecule was calculated using the same method previously used B3LYP / 6-311G (d, p). MEP is a method of correlating electronegativity and partial charges with the chemical reactivity of molecules [32]. It is a three-dimensional visualization that makes it possible to understand the net electrostatic effect of a molecule by means of a graphical representation of the electrostatic potential mapped in the constant electron density surface. It also serves to study and confirm the relative polarity of the compounds. The electrostatic potential values at the surface are represented by different colors. The color code of the map is in the range between −5.459 e−2 (deepest red) and 5.459 e−2 (deepest blue); where red color denotes the negative electrostatic potential or electron rich area and blue region corresponds to the positive electrostatic potential or electron deficient region.

It is understood from the MEP map (Figure 5) that hydrogen atoms of phenyl and nitrogen group exhibit electropositive, this indicates that this group can act as a good donor which consequently expected to be vulnerable site for nucleophilic attack. On the other hand, the negative electrostatic potential region is mainly localized on the groups located on the other side of the molecule especially in the bromine groups, which is possible site for electrophilic attack.

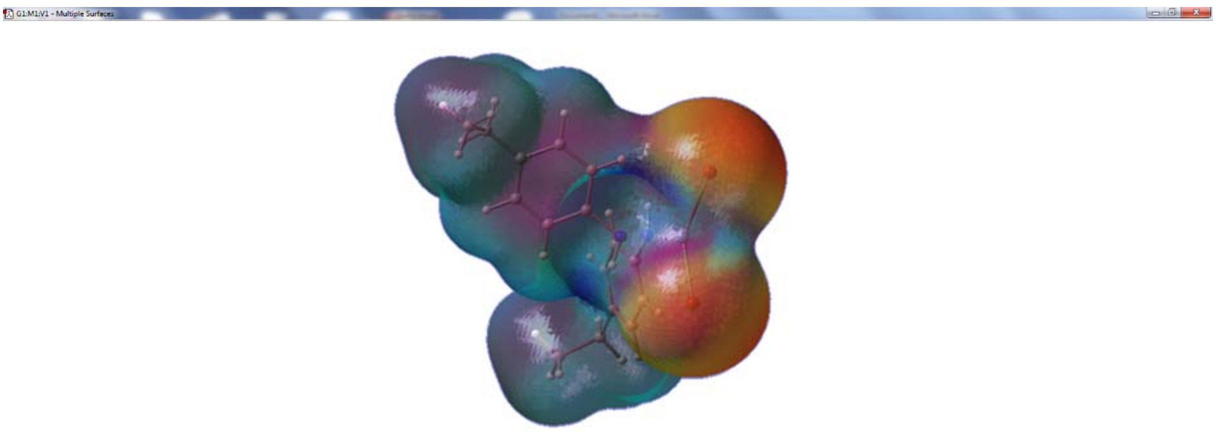

Figure5: Molecular Electrostatic Potential Maps of 4EA-ZnBr2 (Fused system) showing the blue and red color as the positive and negative potential respectively and the green color indicates the intermediate region.

4. Confrontation between the theoretical and experimental results

4.1 Molecular geometry

A comparison between the calculated selected parameters and the experimental data [2] was done to validate the theory level used. The molecular structure of the studied compound (Figure 6), along the c-axis has a form as V, which constitutes two benzene rings, with an angle α between the two planes (P1^P2) of the benzene rings of about 86.22° for the experimental one, and 66.22° for theoretical one. The experimental and theoretical length of the molecule (L) along the crystallographic b axis were found to be 14.85 Å and 14.13 Å respectively.

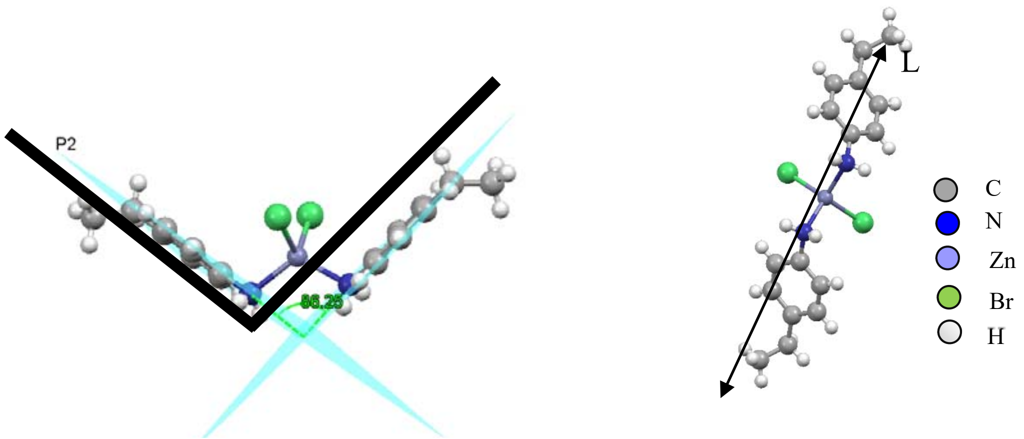

Figure 6: Optimized and experimental molecular structure of 4EA-$ZnBr_2$ along the c-axis and b-axis (α: angle between the two planes P1et P2/ L: length of molecule).

The experimental bonds values C(4)-C(7) (1.5 Å) and C(7)-C(8) (1.39 Å) are in good agreement with the calculated bonds 1.51, and 1.54 Å respectively. The corresponding distances and angles values around the zinc atom in N-Zn, Br-Zn, N1-Zn-N2, Br1-Zn-Br2, N1-Zn-Br2 and C1-N1-Zn are also similar. In addition, the angles C2-C1-N1, C6-C1-N1, C3-C4-C7, C5-C4-C7 and C8-C7-C4 have the same values in both experimental and theoretical studies. However, we have not observed any significant changes in intermolecular distances and angles between the theory and the experimental, except for torsion angles which are 131° and -50° for the experimental C3-C4-C7-C8 and C5-C4-C7-C8, and 90° and -87.63° for the corresponding calculated torsions angles. The intermolecular interactions are represented in the π stacking along the c-axis by the distance CH ... C, and the interaction along the b-axis, which is called side by side, by the distance NH ... Br. Both interactions are hydrogen interactions that have the same experimental and theoretical values. The results are recapitulated in the Table 3.

Table 3: Summarizes the selected parameters obtained at the level of the theory B3LYP / 6-311- G (d, p) and those of SCXRD for the molecule 4EA-ZnBr2.

Complex formula	**$(C_2H_5\text{-}C_6H_4\text{-}NH_2)_2ZnBr_2$**	
	Experimental(SCXRD)	**Theory (TD/DFT)**
The interactions (NH…Br)	2.73/ 2.81 Å	2.70/2.80 Å
The interactions (C-H…C)	2.79Å	2.85 Å
N-Zn	2.05 Å	2.14 Å
Br(2)-Zn(1)	2.38 Å	2.34 Å
N(1)-C(1)	1.45 Å	1.44 Å
C(4)-C(7)	1.50 Å	1.51 Å
C(7)-C(8)	1.39 Å	1.54 Å
N1-Zn-N2	115.85°	101.17°
Br1-Zn-Br2	110.56°	107.21°
N(1)-Zn(1)-Br(2)	108.28°	112.85°
N(1)#1-Zn(1)-Br(2)	106.96°	109.88°

C(1)-N(1)-Zn(1)	113.70°	109.88°
C(2)-C(1)-N(1)	121.60°	120.22°
C(6)-C(1)-N(1)	118.50°	118.77°
C(3)-C(4)-C(7)	122.10°	120.51°
C(5)-C(4)-C(7)	120.30°	120.75°
C(8)-C(7)-C(4)	117.20°	112.37°
C(3)-C(4)-C(7)-C(8)	131.00°	90.53°
C(5)-C(4)-C(7)-C(8)	-50.00°	-87.63°
α (P1^P2)	86.22°	66.00°
L	14.85 Å	14.13 Å

4.2. Optical properties

The comparison between the experimental and theoretical spectra evidences good agreements, but also some discrepancies. The intense absorption peak measured at 236 nm is in good agreement with the calculated peak at 236.54 nm which is due to (π→π*) electronic transition originating in the excitation from the highest occupied molecular orbital (HOMO-2) to the second level of unoccupied molecular orbital LUMO+1. The second experimental peak at 275 nm significantly deviates from the calculated peak at 294 nm which is due to HOMO-10→ LUMO electronic transition. The HOMO-10 and LUMO have large contributions from the n and π* respectively of the ligand 4-Ethylaniline.

An intense calculated absorption band with a maximum at 347.72 nm, slightly different from the experimental maximum at about 338 nm, corresponds to the excitation from HOMO-9 equivalent of t2g6 (ZnII) to the second level LUMO (π*) orbital of 4-Ethylaniline, this absorption band is due to the transition metal-ligand charge-transfer (MLCT).

The other two electronic transitions calculated at 445.21 nm and 604 nm correspond to those observed experimentally at 425nm and 580 nm respectively, showing slight discrepancies between calculation and observation. The first transition corresponds to the excitation from HOMO-8 to the LUMO accompanying the 3p-MO of Br to the 4s-MO of Zn, and the second transition corresponds to the excitation from HOMO-2 (3p of Br) to the LUMO (4p of Zn). The observed differences are probably due to the nature of the investigated sample. The latter is in the form of single-crystals, the molecular structure is therefore impacted, at some extend, by the crystal packing.

Despite the above slight differences, the calculated band gap Eg= 2.22 eV is close from that obtained by experimental UV–VIS spectrum (Eg= 2.15eV). The slight difference between these values can also probably be attributed to the fact that DFT calculations are performed for gas phases and not for solids. Disorganized system tends to increase the gap value while in the solid state the system is organized in most cases as crystals and the value of the band gap is expected slightly lower than that obtained from quantum calculations as found in the present study; note that the difference of 0.07 eV between gas and solid phases band gap energies agrees with the value reported in the literature [33- 36].

5. Conclusions

An experimental and theoretical comparative study of optical features of the complex (CH_3-CH_2-C_6H_4-NH_2)$_2ZnBr_2$, has been carried out, using experimental UV-Vis spectroscopy and TD-DFT-B3LYP theory. The experimental energy gap is found to be 2.15 eV, in good

agreement with the calculated value (2.22 eV), which reveals that the studied complex presents a semiconductor character. Consequently, this kind of material appears of interest to give a new access in the researching field of semiconductor materials. Incidentally, the comparison between the theoretical and experimental values gives also a comparison between the gas phase and the solid phase, for this compound. The studied molecule provides similar features at the level of the absorption bands and the gap in energy of molecules studied in gas and in solid. Some differences can be noted, but globally this molecule adopts a similar behaviour in solid and in gas phases. At the level of the geometric correlation of the molecular, we can notice that the molecule is moving a little when it passes from the solid state to the gas state. This change of state is the cause of finding some different geometrical parameter between the theory and the experimental one, like the angles of torsion formed between C (3) -C (4) -C (7) -C (8) and C (5) -C (4) -C (7) -C (8), as well as for the angle α (P1 ^ P2). The other geometrical parameters are close between the values in gas phase (theory) and in solid phase (experimental). We conclude that the correlation between the theory and the experimental shows that the molecule keeps the same optical properties despite its small difference at the structural level.
On the other hand, the molecular electrostatic potential (MEP) calculation showed that the hydrogen atoms of phenyl and nitrogen group can act as a good donor which consequently expected to be vulnerable site for nucleophilic attack. While the negative electrostatic potential region is mainly localized in the bromine groups, which is possible site for electrophilic attack.

References

[1] Houel, A. (2011). Revêtements polyesters hybrides organiques-inorganiques par voie sol-gel (Doctoral dissertation, INSA de Lyon).

[2] Harmouzi, A., Daro, N., Guionneau, P., Belaaraj, A., & Khechoubi, E. M. (2017). Journal of Crystal Growth.

[3] Travis, W., Knapp, C. E., Savory, C. N., Ganose, A. M., Kafourou, P., Song, X, ... & Palgrave, R. G. (2016). Inorganic chemistry, 55(7), 3393-3400.

[4] Cheetham, A. K., Rao, C. N. R., & Feller, R. K. (2006). Chemical communications, (46), 4780-4795.

[5] C. Sanchez, B. Julian, P. Belleville, M. Popall. J. Mater. Chem. 15 (35–36) (2005) 3559–3592.

[6] X.-H. Lv, W.-Q. Liao, P.-F. Li, Z.-X. Wang, C.-Y. Mao, Y. Zhang. J. Mater. Chem. C 4 (9) (2016) 1881–1885.

[7] X. Guo, C. McCleese, C. Kolodziej, A.C. Samia, Y. Zhao, C. Burda. Dalton Trans. 45 (9) (2016) 3806–3813.

[8] Fukui, K. (1982). 218(4574), 747-754.

[9] Padmaja, L., Ravikumar, C., Sajan, D., Hubert Joe, I., Jayakumar, V. S., Pettit, G. R., & Faurskov Nielsen, O. (2009). Journal of Raman Spectroscopy, 40(4), 419-428.

[10] Ravikumar, C., Joe, I. H., & Jayakumar, V. S. (2008). Chemical physics letters, 460(4), 552-558.

[11] Fleming, I. (2011). John Wiley & Sons.

[12] Baikie, T., Fang, Y., Kadro, J. M., Schreyer, M., Wei, F., Mhaisalkar, S. G, ... & White, T. J. (2013). Journal of Materials Chemistry A, 1(18), 5628-5641.

[13] Kubelka P, Munk F. Zeitschrift Für Technische Physik 1931;12:593.

[14] Jin, J., Han, X., Meng, Q., Li, D., Chi, Y. X., & Niu, S. Y. (2013). Journal of Solid State Chemistry, 197, 92-102.

[15] Lever, A. B. P. (1990). Inorganic Chemistry, 29(6), 1271-1285.

[16] Curtis, J. C., Sullivan, B. P., & Meyer, T. J. (1983). Inorganic Chemistry, 22(2), 224-236.

[17] Yang, J. S., Lin, Y. D., Lin, Y. H., & Liao, F. L. (2004). The Journal of organic chemistry, 69(10), 3517-3525.

[18] Abid, H., Samet, A., Dammak, T., Mlayah, A., Hlil, E. K., & Abid, Y. (2011). Journal of Luminescence, 131(8), 1753-1757.

[19] Zheng, Y. Y., Wu, G., Deng, M., Chen, H. Z., Wang, M., & Tang, B. Z. (2006). Thin Solid Films, 514(1), 127-131.

[20] Xiao, Z. L., Chen, H. Z., Shi, M. M., Wu, G., Zhou, R. J., Yang, Z. S., ... & Tang, B. Z. (2005). Materials Science and Engineering: B, 117(3), 313-316.

[21] Hao, F., Stoumpos, C. C., Cao, D. H., Chang, R. P., & Kanatzidis, M. G. (2014). Nature Photonics, 8(6), 489-494.

[22] Ekström, U., Visscher, L., Bast, R., Thorvaldsen, A. J., & Ruud, K. (2010). Journal of chemical theory and computation, 6(7), 1971-1980.
[23] Becke, A. D. (1993). J. Chem. Phys. 98, 5648–5652.
[24] Lee, C., Yang, W., & Parr, R. G. (1988). Physical review B, 37(2), 785.
[25] Becke, A. D. (1992). The Journal of chemical physics, 96(3), 2155-2160.
[26] Mbarek M., Chemek M., Wery J., Duvail J.L., Alimi K. (2014). Journal of Physics and Chemistry of Solids, 75(6), 752-758.
[27] Hariharan, P. C., & Pople, J. A. (1973). Theoretica chimica acta, 28(3), 213-222.
[28] Lu, X., Wu, C. M. L., Wei, S., & Guo, W. (2009). The Journal of Physical Chemistry A, 114(2), 1178-1184 and references therein.
[29] Gross, E. K., Dobson, J. F., & Petersilka, M. (1996).Density functional theory II (pp. 81-172). Springer, Berlin, Heidelberg.
[30] Frisch, M., Trucks, G. W., Schlegel, H., Scuseria, G. E., Robb, M. A., Cheeseman, J. R., ... & Millam, J. M. (2008). Gaussian 03, revision C. 02.
[31] Gorelsky, S. I. (2010). SWizard program. University of Ottawa, Ottawa, Canada.
[32] Chengjun W., Weibin X., Linwei L., Wei L., Jian W., Tiemin S. (2019). Journal of Molecular Structure, 1175 (5) 638-647.
[33] Ling, L., & Lagowski, J. B. (2013). Polymer, 54(10), 2535-2543.
[34] Eslamibidgoli, M. J., & Lagowski, J. B. (2012). The Journal of Physical Chemistry A, 116(43), 10597-10606.
[35] Salzner, U., Lagowski, J. B., Pickup, P. G., & Poirier, R. A. (1998). Synthetic Metals, 96(3), 177-189.
[36] Naghavi, S. S., Gruhn, T., Alijani, V., Fecher, G. H., Felser, C., Medjanik, K., ... & Baumgarten, M. (2011). Journal of Molecular Spectroscopy, 265(2), 95-101.